Title

Comparison of non-invasive MRI measurements of cerebral blood flow in a large multisite cohort

Journal

Cerebrovascular and Brain Metabolism Reviews, 36(7)

ISSN

1040-8827

Authors

Dolui, Sudipto
Wang, Ze
Wang, Danny JJ
et al.

Publication Date

2016-07-01

DOI

10.1177/0271678x16646124

Peer reviewed

Original Article

JCBFM

Journal of Cerebral Blood Flow & Metabolism
0(00) 1–13

DOI: 10.1177/0271678X16646124
jcbfm.sagepub.com

SAGE

Comparison of non-invasive MRI measurements of cerebral blood flow in a large multisite cohort

Sudipto Dolui[1,2,3], Ze Wang[4,5], Danny JJ Wang[6], Raghav Mattay[7], Mack Finkel[8], Mark Elliott[1], Lisa Desiderio[1], Ben Inglis[9], Bryon Mueller[10], Randall B Stafford[11], Lenore J Launer[12], David R Jacobs, Jr[13], R Nick Bryan[1] and John A Detre[1,2,3]

Abstract

Arterial spin labeling and phase contrast magnetic resonance imaging provide independent non-invasive methods for measuring cerebral blood flow. We compared global cerebral blood flow measurements obtained using pseudo-continuous arterial spin labeling and phase contrast in 436 middle-aged subjects acquired at two sites in the NHLBI CARDIA multisite study. Cerebral blood flow measured by phase contrast (CBF_{PC}: 55.76 ± 12.05 ml/100 g/min) was systematically higher ($p < 0.001$) and more variable than cerebral blood flow measured by pseudo-continuous arterial spin labeling (CBF_{PCASL}: 47.70 ± 9.75). The correlation between global cerebral blood flow values obtained from the two modalities was 0.59 ($p < 0.001$), explaining less than half of the observed variance in cerebral blood flow estimates. Well-established correlations of global cerebral blood flow with age and sex were similarly observed in both CBF_{PCASL} and CBF_{PC}. CBF_{PC} also demonstrated statistically significant site differences, whereas no such differences were observed in CBF_{PCASL}. No consistent velocity-dependent effects on pseudo-continuous arterial spin labeling were observed, suggesting that pseudo-continuous labeling efficiency does not vary substantially across typical adult carotid and vertebral velocities, as has previously been suggested. Conclusions: Although CBF_{PCASL} and CBF_{PC} values show substantial similarity across the entire cohort, these data do not support calibration of CBF_{PCASL} using CBF_{PC} in individual subjects. The wide-ranging cerebral blood flow values obtained by both methods suggest that cerebral blood flow values are highly variable in the general population.

Keywords

Cerebral blood flow, labeling efficiency, phase contrast magnetic resonance imaging, pseudo-continuous arterial spin labeling, semi-automated vessel segmentation

Received 30 November 2015; Revised 21 March 2016; Accepted 22 March 2016

[1]Department of Radiology, University of Pennsylvania, Philadelphia, PA, USA
[2]Department of Neurology, University of Pennsylvania, Philadelphia, PA, USA
[3]Center for Functional Neuroimaging, University of Pennsylvania, Philadelphia, PA, USA
[4]Center for Cognition and Brain Disorders and the Affiliated Hospital, Hangzhou Normal University, Hangzhou, China
[5]Departments of Psychiatry and Radiology, Perelman School of Medicine, University of Pennsylvania, Philadelphia, PA, USA
[6]Department of Neurology, University of California, Los Angeles, CA, USA
[7]Raymond and Ruth Perelman School of Medicine, University of Pennsylvania, Philadelphia, PA, USA
[8]School of Arts and Sciences, University of Pennsylvania, Philadelphia, PA, USA
[9]Henry H. Wheeler Jr. Brain Imaging Center, University of California, Berkeley, CA, USA
[10]Department of Psychiatry, University of Minnesota, Minneapolis, MN, USA
[11]Department of Clinical Neurosciences, University of Calgary, Calgary, Alberta, Canada
[12]Laboratory of Epidemiology and Population Science, National Institute on Aging, Bethesda, MD, USA
[13]Division of Epidemiology and Community Health, University of Minnesota, Minneapolis, MN, USA

Corresponding author:
John Detre, Departments of Neurology and Radiology, University of Pennsylvania, 3 W Gates Pavilion, 3400 Spruce Street, Philadelphia, PA 19104, USA.
Email: detre@mail.med.upenn.edu

Introduction

The brain represents about 2% of body weight, but is one of the most highly perfused organs in the body, utilizing approximately 15% of the cardiac output and 20% of the total body oxygen.[1] Cerebral blood flow (CBF)[2,3] is classically defined in tissue-specific units (ml of blood/100 g brain tissue/min) and it is widely accepted that mean global CBF in healthy subjects is on the order of 50 ml/100 g/min.[4] As major reductions in CBF are the primary cause of stroke, CBF provides a direct biomarker for cerebrovascular function and health. In addition, CBF is closely coupled to brain metabolism and hence provides a surrogate marker of brain function.[5]

Arterial spin-labeled (ASL) perfusion magnetic resonance imaging (MRI) provides a non-invasive method for quantifying whole-brain and regional CBF by using magnetically labeled arterial blood water as a nominally diffusible perfusion tracer.[6–10] The perfusion is proportional to the difference of two images obtained with and without labeling (referred as labeled or tagged image and control image respectively) and can be converted to absolute CBF using specific models[10,11] and assumptions. Signal-to-noise ratio (SNR) presents a challenge to accuracy of the ASL estimate of CBF, requiring averaging of multiple label/control image acquisitions to increase SNR. There are several variations of ASL based on the method of labeling the arterial blood water.[6,7,12–14] Pseudo-continuous ASL (PCASL)[14] is presently the recommended optimal labeling strategy[13] because of its compatibility with modern MRI hardware and higher SNR compared to alternative options.

Phase contrast (PC)[15–17] MRI provides an alternative non-invasive method for estimating whole-brain average CBF based on measurement of blood flow through the internal carotid arteries (ICAs) and vertebral arteries (VAs), which supply blood to the brain. PC measures the velocity of blood through a blood vessel using a bipolar gradient (two symmetric lobes with equal area) to encode flow by inducing phase shifts that are proportional to the flow velocity, and a flow compensated gradient for control acquisition. Subsequently, the total flow rate is obtained by integrating the flow velocities across the four arteries supplying blood to the brain, while a structural MRI scan is used to quantify the brain volume to derive whole-brain CBF in ml/100 g/min. Regional CBF cannot be measured with PC.

An important parameter in the quantification of CBF in ASL is the labeling efficiency, which refers to the degree of magnetic inversion for blood water flowing through the tagging plane.[14,15] While PCASL is designed to invert flowing blood water over a range of velocities,[14] it is nonetheless sensitive to arterial velocity, which can be affected by vessel orientation or stenosis, and to other biophysical factors such as RF and magnetic field inhomogeneity at the labeling plane. Protocols for assessing vessel anatomy and signal quality at the labeling plane have been devised to optimize PCASL labeling efficiency,[18] but these are cumbersome to perform and as a result, an assumed labeling efficiency of 0.8–0.85 is often used[13] in routine practice. One way of assessing labeling efficiency is to compare CBF assessed by PCASL with an independent measure of CBF, such as PC, and comparisons between PCASL and PC acquired concurrently have been used to assess PCASL labeling efficiency[15,19] and calibrate the CBF measurements. However, this approach is based on the assumption that CBF assessed by PC is accurate.

The aim of the present study was to compare and cross-validate whole-brain CBF measurements obtained using PCASL MRI (referred below as CBF_{PCASL}) and PC (referred below as CBF_{PC}) from a large cohort of typical middle-aged subjects scanned as part of the multisite coronary artery risk development in young adults (CARDIA) study. This comparison is intended to provide insights into CBF variability based on methods that can readily be applied in a population-based study. Using data from over 500 subjects, we measured and compared the range and variability of CBF based on these two independent measurement strategies. In addition, we compared the CBF values obtained from the two non-invasive methods. We also investigated the rationale of using CBF_{PC} to calibrate CBF_{PCASL}, since prior work suggested that PC could be used to correct for inter-subject variations in labeling efficiency in PCASL.[15] Toward this end, we assessed whether the variability in CBF_{PCASL} measurements could be completely described by the CBF_{PC} measurements, and whether the PCASL labeling efficiency, computed as a ratio of the CBF_{PCASL} and CBF_{PC}, varies significantly as a function of arterial velocity, which was previously proposed as the main source of variations in labeling efficiency. In lieu of a "gold standard" measure of quantitative CBF, we assessed age and gender effects, which are known modulators of CBF,[20,21] as another means of comparing PCASL and PC.

Materials and methods

Cohort

CARDIA is a multisite, longitudinal study aiming at examining the development and determinants of clinical and subclinical cardiovascular disease. MRI data acquired at two sites (Minneapolis and Oakland) from 541 (291 from the Minneapolis site and 250 from the

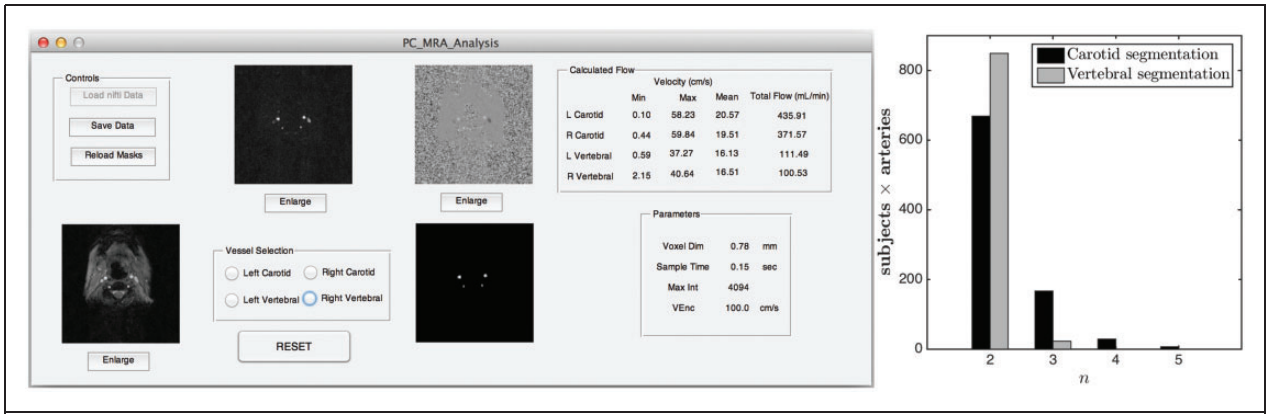

Figure 1. (Left subplot) A screen shot of the PC utility developed in MATLAB; (Right subplot) distribution of the value of *n* (number of standard deviation of noise for setting the threshold to segment the arteries) for carotid and vertebral segmentations.

Oakland site) healthy middle-aged subjects, including blacks and whites and males and females aged 43–56 years, who underwent the MRI protocol of CARDIA Year 25 on 3 Tesla Siemens MRI scanners were considered for this study. The MRI protocols in Minneapolis and Oakland were approved by the Institutional Review Board of the University of Minnesota and the Kaiser Permanente Northern California (KPNC) Institutional Review Board, respectively. Institutional Review Boards in the United States adhere to the ethical principles and guidelines for the protection of human subjects in research enumerated in the Belmont Report (http://www.hhs.gov/ohrp/humansubjects/guidance/belmont.html), produced by the National Commission for the Protection of Human Subjects of Biomedical and Behavioral Research (April 1979). All participants signed written informed consent for the brain MRI and for all other CARDIA procedures. The data used in this study and all CARDIA data are available through the CARDIA Coordinating Center (http://www.cardia.dopm.uab.edu/contact-cardia) after approval of a paper proposal submitted to the CARDIA Publications and Presentations Committee.

Image acquisition

Non-background-suppressed PCASL data were acquired using gradient-echo echoplanar imaging (EPI) with the following parameters: TR/TE: 4 s/11 ms, voxel size: $3.4 \times 3.4 \times 5$ mm^3, matrix $= 64 \times 64$, flip angle $= 90^\circ$, FOV $= 220$ mm, bandwidth $= 3004$ Hz/pixel, echo spacing $= 0.44$ ms and EPI factor $= 64$. Twenty slices with a distance factor of 20% were acquired from inferior to superior in a sequential order. PCASL was performed with labeling offset $= 90$ mm, duration $= 1.48$ s, post-labeling delay (PLD) $= 1.5$ s, RF gap $= 0.36$ ms, RF duration $= 0.5$ ms and mean $G_z = 0.6$ mT/m. 40 label and control pairs were acquired. The PC data were acquired at eight phases within a cardiac cycle with a maximum velocity encoding of 100 cm/s. Other PC acquisition parameters were: voxel size: $0.8 \times 0.8 \times 5.0$ mm^3, FOV: 20 cm, TR $=$ 140 ms, TE $= 10$ ms, flip angle $= 15^\circ$, and bandwidth $=$ 260 Hz/pixel. PC imaging was performed near the PCASL labeling plane.[22] PCASL and PC scans were performed in a fixed order (PCASL followed by PC). The scan protocol included a T1-weighted 3D MPRAGE sequence used for segmentation of different tissues and for computing the total brain volume. This scan was sagittally acquired with the following parameters: resolution: $1 \times 1 \times 1$ mm^3, TR/TE/TI $= 1900/2.9/900$ ms, matrix $= 256 \times 256$, slices $= 176$, FOV $=$ 250 mm, flip angle $= 9^\circ$, GRAPPA $= 2$, and bandwidth $= 170$ Hz/pixel.

Processing of PC data using an in-house MATLAB program – PC analysis utility

All PC data were analyzed by a single author (R.M.) using an in-house developed MATLAB (The Mathworks Inc., Natick, MA) program equipped with (i) semi-automated vessel segmentation and (ii) the function for visualizing the flow velocity profile. A snapshot of the utility is shown in the left subplot of Figure 1. The segmentation process used a pixel-wise maximum of the eight complex difference images (corresponding to eight phases) of the PC data. The user selects a particular artery by clicking inside it. Thereafter, the ROI is grown iteratively by comparing the intensities of all unallocated neighboring pixels to a threshold and adding to the ROI those pixels whose intensities are above threshold. Such a region-growing approach has the advantage of resulting in a connected ROI. The threshold was set to n times the noise level, where $n = 2$ by default, and could be modified by the

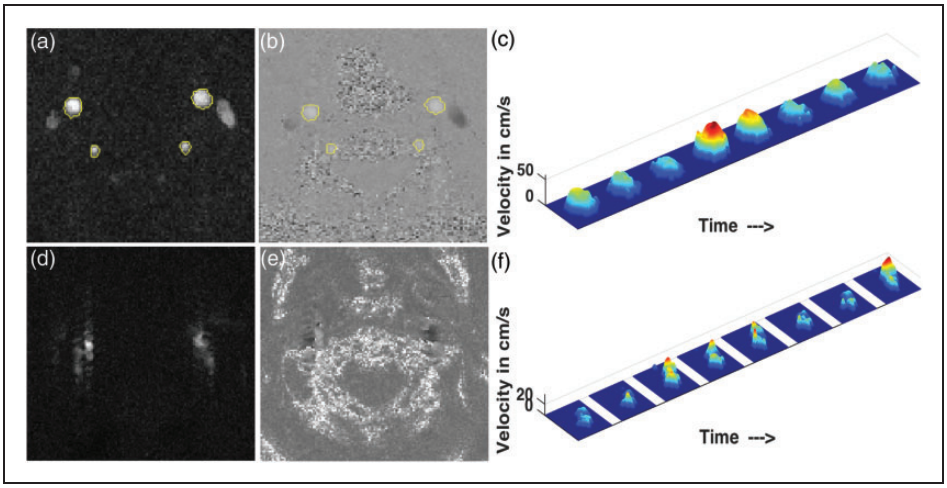

Figure 2. Segmentation in PC (a) complex difference and (b) phase image of a particular subject; (c) velocity profile of the left carotid artery of the same subject. (d) Example of complex difference image of poor quality, (e) corresponding phase image and (f) the velocity profile of the left carotid for the same subject.

user in the case of unsatisfactory segmentation. The noise level was estimated as the median of the intensities of the complex difference image. The right subplot of Figure 1 shows the distribution of n for the ICAs and the VAs. From the distribution, it can be seen that $n = 2$ was effective in vast majority of cases. Once the initial automatic segmentation is done, the user has the option of manually editing the segmentation by clicking on the image to add or remove particular pixels from the ROI in the case of an obvious error, though this was not required for the results shown in this study. Figure 2(a) and (b) shows the segmentation results on the complex difference and phase image of a particular subject.

Once the segmentation mask is obtained, the velocity of the blood flow for each of the eight phases at each voxel is obtained as

$$\upsilon = \frac{2\upsilon_{\text{enc}}\phi}{\phi_{\max}} - \upsilon_{\text{enc}}$$

where υ_{enc} is the velocity encoding (100 cm/s), and ϕ and $\phi_{\max}$ are the voxel-intensity and the maximum intensity (4095) of the phase images, respectively. The segmentation mask is further refined by restricting the ROI only to those voxels for which the mean velocity values across the eight phases are positive. This step ensures that the veins, which also appear bright in the complex difference image and may be located immediately next to the arteries, are excluded from the mask. Although this step can potentially overestimate the flow values by eliminating the noisy negative voxels from the averaging process, any such exclusion of voxels is expected to happen at the edges and hence the bias should be small. The velocity is subsequently converted to volume flow rate (VFR), denoted by F, by integrating the velocity over the cross-sectional area given by

$$F = \int \upsilon \mathrm{d}A$$

The MATLAB program also can display the velocity profiles for the user to determine whether the flow is laminar or non-laminar. An example of the laminar velocity profile for all the eight phases is shown in Figure 2(c). PC data quality was rated as "good," "non-laminar," or "poor" for each artery based on the segmentation masks, VFR values, and visualization of the velocity profiles. We compared velocity histograms for "good," "non-laminar," and "poor" flow patterns for both ICAs and VAs and determined that there was no difference in flow distributions between "good" and "non-laminar" patterns (data not shown). Accordingly, both "good" and "non-laminar" ratings were considered as acceptable measures of arterial flow, whereas cases with "poor" flow patterns were removed. The total blood VFR was obtained by adding the individual VFRs through the ICAs and VAs. Subsequently, CBF_{PC} is obtained by dividing the total blood VFR by the product of the brain volume (grey matter and white matter volume) and the brain density (assumed to be 1.06 g/ml[15]). The brain volume was obtained by the following steps: (i) segmenting the high-resolution T1-weighted 3D MPRAGE data using the "new segment" in SPM8 (Wellcome Department of Imaging Neuroscience, London, UK) to obtain the tissue probability maps (ii) thresholding the sum of the obtained gray matter and white matter tissue probability maps to 0.2 to obtain the brain mask, and finally

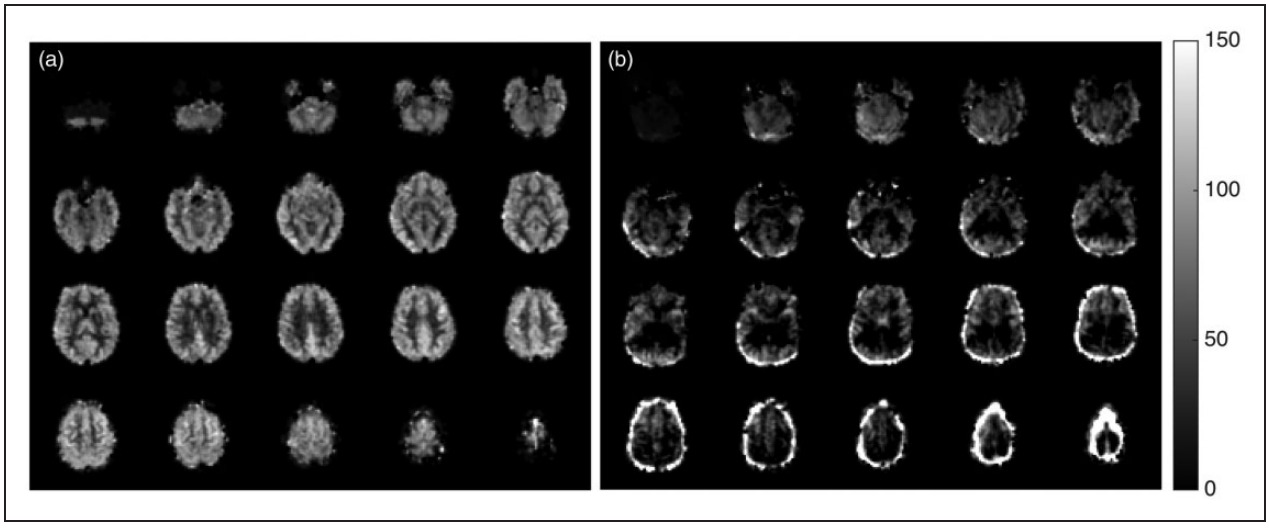

Figure 3. (a) Representative CBF_{PCASL} map in the study sample (b) Example of CBF_{PCASL} map of poor quality (shows extensive negative CBF values and high values at the edge of the brain suggestive of motion artifacts).

(iii) multiplying the total number of voxels within the mask by the volume of each voxel.

In addition to computing the average CBF_{PC}, the average flow velocity through the four arteries was computed as

$$\upsilon_{\text{avg}} = \frac{\sum_{i=\text{ICAs and VAs}} \upsilon_i F_i}{\sum_{i=\text{ICAs and VAs}} F_i}$$

where υ_i and F_i are the average velocity and the VFR, respectively, through the ith artery, the subscript i being the two internal carotid and VAs. In other words, the average flow velocity is computed as the weighted average of the flow velocity through each contributing artery, where the weights are proportional to the amount of blood flowing through that artery. Following a similar procedure, weighted average of maximum velocity was also computed, where the υ_i is made equal to the maximum velocity through the ith artery.

Processing of PCASL images

ASL data were processed using ASLtoolbox,[23] which is based on SPM8. The processing consists of first aligning the raw EPI images using a six-parameter rigid body motion spatial transformation. The spurious motion component caused by the systematic label/control alternation was regressed out from the motion parameters using the method in Wang[24] before applying the transformation on the images. This was followed by the removal of residual motion.[24] Subsequently, each volume in the time series was smoothed using a isotropic Gaussian kernel with a full-width-half-max (FWHM) = 5 mm. Pairwise subtraction of the resulting images was performed and the difference was converted to absolute CBF measurements using the formula[13,25]

$$CBF(\text{ml}/100\text{g}/\text{min}) = \frac{60 \times 100\lambda\Delta M e^{\omega/T_{1blood}}}{2\alpha T_{1,blood} M_0 (1 - e^{-\tau/T_{1blood}})}$$

where ΔM is control-label difference, λ is the blood: brain partition coefficient, ω is the PLD, $T_{1,blood}$ is the T_1 of blood, α is the labeling (tagging) efficiency, M_0 is the equilibrium magnetization of the brain, and τ is the labeling duration. In the present work, $\lambda = 0.9$ ml/g, $\omega = 1.5$ s, $T_{1,blood} = 1664$ ms, $\alpha = 0.85$, M_0 is considered to be equal to the corresponding control image and $\tau = 1.48$ s. Each subject's CBF volume was obtained by computing the average of the time series. An example of a mean CBF map is shown in Figure 3(a). Finally, the mean global CBF (CBF_{PCASL}) for individual subjects was computed by finding the average of the CBF values of the whole-brain (gray matter and white matter only). This whole-brain mask was obtained by first segmenting the high-resolution T1-weighted image using the SPM8 "new segment" method to obtain the tissue probability maps, coregistering them to the functional space, adding the tissue probability maps of the gray matter and the white matter, and finally thresholding the result to 0.85. Note that this mask was intended to minimize CSF partial volume contamination of brain voxels in relatively low resolution PCASL data, and hence uses a higher brain composition threshold than the whole-brain mask used in PC-MRI that was used to obtain the total volume of the brain.

Data QA

PC data from 83 subjects were discarded due to poor flow patterns rendering PC velocities questionable, imaging below the carotid bifurcation (which would include external carotid flow not contributing to CBF), or other artifacts. An example of a complex difference image and the phase image of poor quality and the velocity profile of the left carotid artery corresponding to the same data are shown in Figure 2(d) to (f), respectively. The PCASL mean CBF maps were visually inspected and data from 29 subjects were discarded due to various artifacts. An example of CBF_{PCASL} volume of poor quality is shown in Figure 3(b). Seven subjects had poor quality of both PCASL and PC data, leaving 436 subjects (219 from the Minneapolis site and 217 from the Oakland site) to be considered for the final analysis.

Details of statistical analyses

Statistical analyses were performed to compare and contrast the CBF measurements obtained using PC and PCASL both for the whole cohort and across sites, and also to assess the effect of arterial blood velocity on the labeling efficiency. The descriptive statistics for the different outcomes of the processed data are also reported.

First, we report the descriptive statistics of the measurements for each of PC and PCASL methods relevant to the present study. In the case of PC, we report VFRs as well as the mean and the maximum velocities in ICAs and VAs. The total VFRs in ICAs and VAs were computed by adding the VFRs in the left and right sides. The mean and the maximum velocities within the Carotid and VAs were computed by a weighted average, where the weights were proportional to the VFR through the contributing arteries as mentioned before. The VFR, mean, and maximum velocities were compared between carotid and VAs. In the case of PCASL, we report the mean and standard deviation for global CBF values ($CBF_{PCASL.}$).

The overall distribution of mean CBFs across the sample was examined to characterize the variability in mean CBF in a healthy study sample and to compare whole-brain CBF across the two independent methods. Their mean values were compared using a paired T test to assess for intermodal differences. CBF variability for each modality was characterized. We also assessed CBF values for each modality for effects of gender and age, which are known modulators of CBF.[20,21] Two sample T tests were used to compare the CBF in male and female population for each method and the correlation of CBF with age was also computed. Thereafter, the effects of age and sex were regressed out and the residual variabilities were compared. CBF values obtained using the two methods were then assessed for agreement by visually inspecting their scatter plot and computing the Pearson's correlation coefficient between the two sets of values. Site effects for both modalities were investigated. Two sample T tests were used to test for differences in mean CBF between the sites for each modality. In addition, F-tests for equality of two variances were used to test for differences in variances between the two sites.

Finally, potential velocity-dependent effects on labeling efficiency were assessed. Following prior work,[15] the ratios of CBF_{PCASL} and CBF_{PC} for individual subjects were considered, though in the present work, CBF_{PCASL} was estimated using an assumed labeling efficiency of 0.85. The ratios for individual subjects were considered as a function of their mean velocities of the arterial blood. To assess for reduced labeling efficiency at increased flow velocities, subjects were divided into two groups based on whether their average flow velocity was less than or greater than 20 cm/s, and two different regression lines for each group were plotted along with computation of their correlation coefficient. This analysis was repeated by replacing the mean velocity with the maximum velocity.

Results

Description of sample

The sample of 541 participants consisted of 53% females, 47% males, mean age 50.4 ± 3.4 years, 63% Caucasians, 37% African Americans, 31% hypertensives (61% of whom were treated), 9% diabetics, 25% former smokers, 16% current smokers, 12% with treated hyperlipidemia, and mean body mass index (BMI) $28.4 \pm 5.5\,kg/m^2$. Corresponding values for the 436 participants included in the analysis were 54% females, mean age 50.4 ± 3.5 years (see Table 1), 64% Caucasians, 26% hypertensives (70% of whom were treated), 7% diabetics, 25% former smokers, 15% current smokers, 15% with treated hyperlipidemia, and mean BMI $28.0 \pm 5.3\,kg/m^2$.

Characterization of arterial flow by PC

The VFR in the ICAs (558.04 ± 135.08 ml/min) was significantly higher (paired $t = 53.8$, $p < 0.0001$) than that in the VAs (202.81 ± 56.37 ml/min). The same was true for the mean and the maximum velocities. Specifically, ICA mean velocity (18.51 ± 3.72 cm/s) was significantly higher (paired $t = 20.1$, $p < 0.001$) than the VA mean velocity (14.10 ± 2.86 cm/s), and the ICA maximum velocity (31.70 ± 7.29 cm/s) was significantly higher (paired $t = 20.5$, $p < 0.0001$) than the VA maximum velocity (21.98 ± 5.19 cm/s). Standard deviations for ICA flow and velocities were generally higher than the VA.

Table 1. Descriptive statistics of CBF_{PCASL} and CBF_{PC} values from PCASL and PC MRI in the study sample ($N = 436$).

	Minneapolis	Oakland	Total
# Subjects	219	217	436
Male (%)	45.66	47.00	46.33
Age in years	50.47 ± 3.37	50.24 ± 3.60	50.35 ± 3.48
(min, max)	(43,56)	(43,56)	(43,56)
CBF_{PCASL}	48.08 ± 10.06	47.32 ± 9.43	47.70 ± 9.75
(min, median, max)	(25.67,48.08,81.99)	(26.53,47.50,75.85)	(25.67,47.94,81.99)
CBF_{PC}	53.34 ± 9.31	58.20 ± 13.89	55.76 ± 12.05
(min, median, max)	(32.42,52.71,87.69)	(31.18,55.35,102.91)	(31.18,53.77,102.91)
CBF_{PCASL} in female	51.49 ± 9.41	50.03 ± 8.84	50.77 ± 9.15
CBF_{PCASL} in male	44.02 ± 9.31	44.25 ± 9.16	44.14 ± 9.21
CBF_{PC} in female	56.37 ± 8.93	62.17 ± 13.60	59.22 ± 11.80
CBF_{PC} in male	49.74 ± 8.47	53.71 ± 12.86	51.75 ± 11.06
CBF_{PCASL}-CBF_{PC} correlation	0.72 ($p < 0.0001$)	0.56 ($p < 0.0001$)	0.59 ($p < 0.0001$)

Note: Mean $\pm$ standard deviation and other statistics as specified.
MRI: magnetic resonance imaging; PCASL: pseudo-continuous arterial spin labeling; CBF: cerebral blood flow.

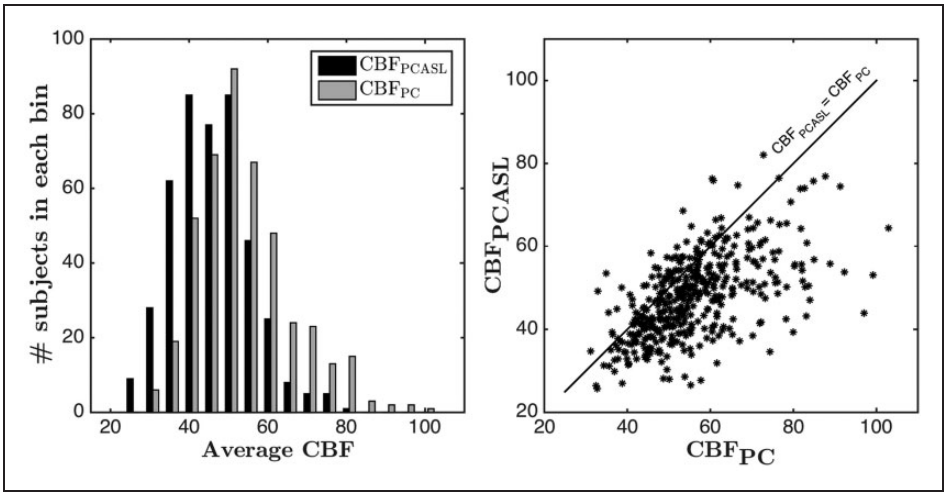

Figure 4. (Left subplot) Histogram of average CBF_{PCASL} and CBF_{PC} values (Right subplot) Scatter plot of CBF_{PCASL} and CBF_{PC} (Pearson's correlation coefficient: 0.59) in individual subjects along with the unity line.

ICA and VA VFRs correlated weakly but significantly ($r = 0.16$, $p = 0.0007$), but no such correlation was observed between their velocities. The average brain volume for the cohort was 1297.86 ± 141.12 cc.

Characterization of CBF measurements by each modality

Across the study sample, average CBF_{PCASL} was 47.70 ± 9.75 ml/100 g/min (Table 1). PC showed a higher average global CBF value of 55.76 ± 12.05 ml/100 g/min ($t = 16.6$, $p < 0.0001$) compared to CBF_{PCASL}. The left subplot of Figure 4 shows the distribution of CBF values obtained using each method. From Figure 4 and Table 1, it can be seen that both methods demonstrate a wide range of CBF values. The range is larger in PC as compared to PCASL. The correlation between CBF_{PCASL} and CBF_{PC} was 0.59 ($p < 0.00001$). A scatter plot showing CBF_{PCASL} versus CBF_{PC} is displayed in the right subplot of Figure 4. For reference, the unity line is also shown on the same plot. CBF_{PC} tended to be higher than CBF_{PCASL} values for most of the subjects.

The mean CBF_{PCASL} in females was significantly higher ($t = 7.53$, $p < 0.0001$) than that of the males (Table 1). The mean CBF_{PC} in females was also significantly higher ($t = 6.79$, $p < 0.0001$) than in males.

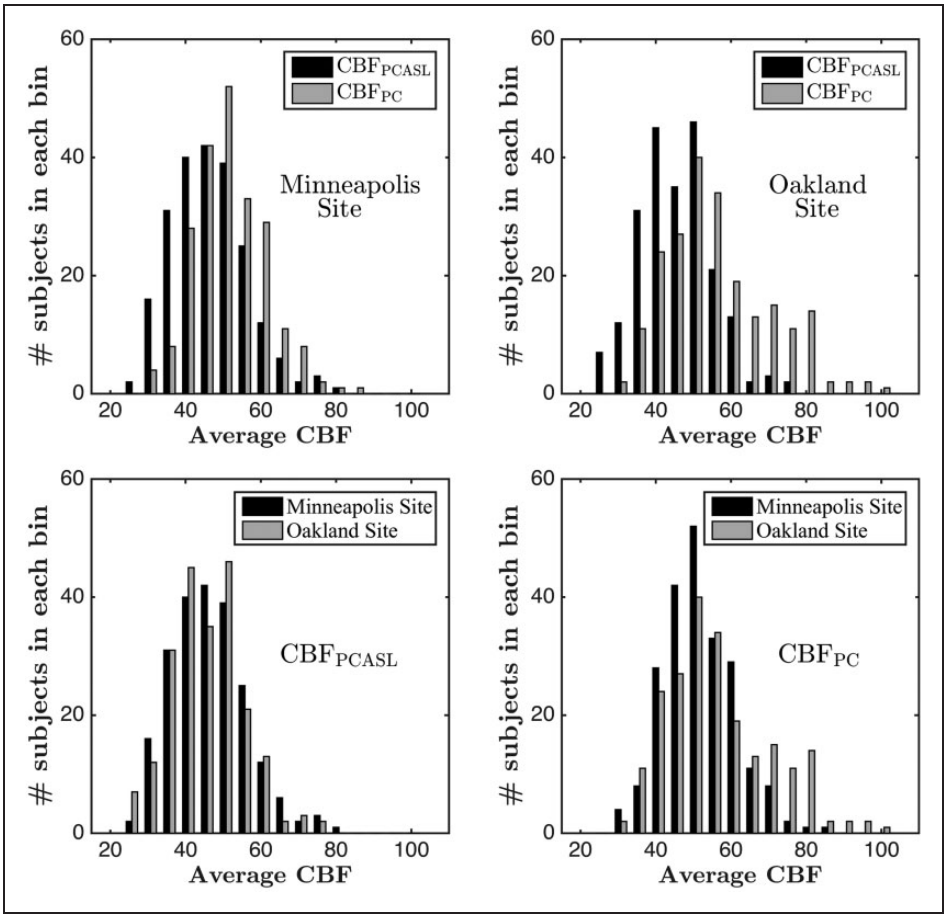

Figure 5. (Top subplots) PCASL versus PC CBF comparison in (top left) Minneapolis and (top right) Oakland sites (Bottom subplots) Cross-site comparison of (bottom left) CBF_{PCASL} and (bottom right) CBF_{PC}.

The correlation between CBF_{PCASL} and age was -0.13 ($p = 0.005$), similar to the correlation for CBF_{PC} with age: -0.11 ($p = 0.021$). We also assessed the residual variability in CBF values after regressing out the effect of age and sex, which have known associations with variability in CBF. The standard deviation decreased from 9.74 to 9.08 ml/100 g/min in the case of CBF_{PCASL} and from 12.05 to 11.39 ml/100 g/min in the case of CBF_{PC}.

Site effects for each modality

All data were acquired at one of two sites with identical scanning hardware. Table 1 shows the descriptive statistics for Minneapolis and Oakland sites. Sample size, age, and sex distribution were well matched across the sites. A graphical representation of site effects is shown in Figure 5. The top two subplots of Figure 5 show the histograms of CBF_{PCASL} and CBF_{PC} for the Minneapolis and Oakland sites, respectively. In both cases, CBF_{PC} is shifted towards the right, though this effect is more prominent in the Oakland site. Variability between the two modalities is also more noticeable in the Oakland site compared to the Minneapolis site. The same conclusions can also be derived from Table 1. The bottom two subplots of Figure 5 show cross-site comparison of histograms of CBF_{PCASL} and CBF_{PC}, respectively. The CBF_{PC} distribution corresponding to the Oakland site is shifted towards right and shows a higher range. On the other hand, CBF_{PCASL} distributions are mostly overlapping. Statistically, CBF_{PC} was significantly higher ($t = 4.29$, $p < 0.0001$) and more variable, with F (216 and 218 df) $= 2.23$, $p < 0.00001$, in the Oakland site than in the Minneapolis site. On the other hand, no significant differences in means and variances of CBF_{PCASL} were found between the two sites. The correlations between CBF_{PCASL} and CBF_{PC} in the two sites were found to be 0.72 and 0.56, respectively, both of them being statistically significant ($p < 0.0001$).

Velocity-dependent effects on PCASL labeling efficiency

The left subplot of Figure 6 shows a scatter plot of the ratio of CBF_{PCASL} and CBF_{PC} versus the mean velocity of the arterial blood. The points are divided into two

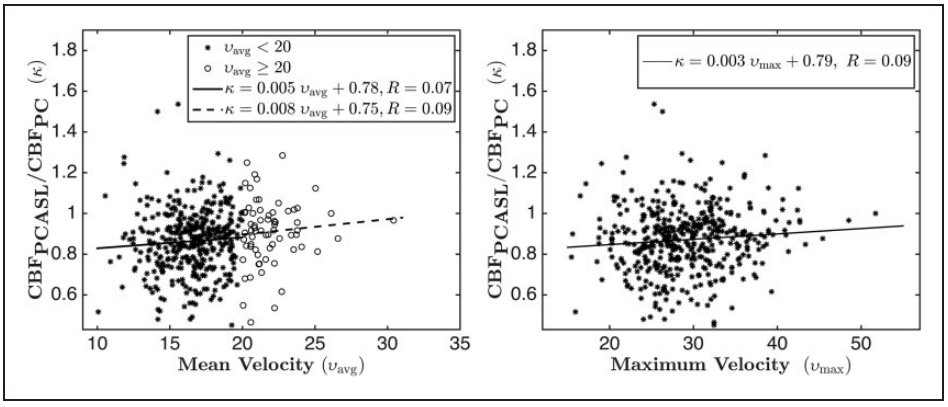

Figure 6. (Left subplot) Scatter plot of the ratio of CBF_{PCASL} and CBF_{PC} with respect to mean flow velocity. The asterisks corresponds to $\upsilon < 20$ cm/s and the circles correspond to $\upsilon > 20$ cm/s. The solid and the dotted lines show fits corresponding to $\upsilon < 20$ cm/s and $\upsilon > 20$ cm/s, respectively. The fit corresponding to the complete data set is $\kappa = 0.007\ \upsilon + 0.75$, $R = 0.13$. (Right subplot) Scatter plot of the ratio of the CBF_{PCASL} and CBF_{PC} with respect to maximum flow velocity; the line shows fit for the complete data set.

subgroups, one with average flow velocity less than 20 cm/s (shown by asterisks) and the other with greater than 20 cm/s (shown by circles). The regression lines for the two subgroups are plotted with solid and dotted lines respectively. The slopes of the two regression lines are almost the same for the two velocities, suggesting that PCASL labeling efficiency, as assessed by comparison with CBF_{PCASL} with CBF_{PC}, does not decrease with increase in mean flow velocity. The correlation in each case was slightly positive, though not statistically significant. However, the correlation for the whole data set was weakly but significantly positive ($r = 0.13$, $p = 0.007$). For further verification, the right subplot of Figure 6 shows the scatter plot of the ratio of the CBF values versus the maximum velocity along with the regression line for the whole data set. The slope of the line is positive, but there was no statistically significant correlation ($r = 0.09$, $p > 0.05$) between the two variables.

Discussion

In a large sample of middle-aged subjects, mean global CBF values by both PCASL and PC were close to the accepted value of 50 ml/100 g/min, but demonstrated a wide range from ~25 ml/100 g/min to ~100 ml/100 g/min. Since the range of variation was consistent across two differing modalities with a highly significant correlation different modalities and remained large after regressing out effects of age and sex, which are known moderators of CBF, the observed distribution in CBF across the cohort is most likely physiological rather than primarily reflecting measurement artifacts. Further research will be needed to elucidate the biological bases for individual differences in CBF, which likely reflect a range of genotype, phenotype, and state-dependent effects.

On a group level, the correlation of the two CBF measurements was found to be substantial. However, for a fixed value of CBF from one modality, the range of CBF values of the other modality was large. On an average about 34% of the CBF_{PCASL} variance could be explained by the CBF_{PC}, but a large amount of residual variability (~66%) remains. In the case of PCASL as implemented in this study, a variety of potential sources of variability can be considered. Variations in labeling efficiency may have occurred due to the variable location of the labeling plane relative to the arterial tree, since this study used a fixed labeling location relative to the imaging volume. In addition, CBF_{PCASL} quantification using the modified single compartment model is dependent on the T1 of blood.[11] This study used a literature value for blood T1,[26] but blood T1 is known to vary as a function of hematocrit and oxygen saturation.[27] A 10% variability in T1 leads to about 11–15% variability in CBF measurements keeping the other parameters fixed. Quantification of mean CBF is also dependent on the segmentation of the T1 scans into different tissue classes and on the coregistration of these segmentations to the functional space. Although, the ''new segment'' algorithm of SPM8 has been shown to provide reliable segmentation accuracy on an average,[28] significant challenges exist on an individual subject level because of individual differences in brain structure. The coregistration process is also prone to errors.[29]

The CBF quantification for individual subjects using PC is dependent on the accuracy of the segmentation of the arteries, errors inherent to the PC MRI techniques, and the estimation of the total brain volume.

Segmentation of the arteries was often challenging when the flow was highly non-laminar or the scan was taken at an oblique angle, and in many cases PC data were deemed unusable. Partial volume effects in PC can cause significant errors in estimation of VFR as reported in prior literatures.[30–32] Other sources of errors in the PC acquisition include mismatch of encoding velocity compared to the true velocity or significant deviations of the imaging plane from orthogonal to the direction of flow.[33] The estimation of total brain volume is also dependent on automatic segmentation algorithm, similar to that used for PCASL quantification. Finally, although CBF is thought to be maintained at a relatively constant value over a wide range of perfusion pressure (by a phenomenon known as cerebral autoregulation),[34] technologies such as transcranial Doppler ultrasonography (TCD)[35] and laser Doppler flowmetry,[36] which allow flow measurements at high-temporal resolution, demonstrate that there are significant variations of the CBF around these steady state values.[37] For this study, the PC scans were acquired from only eight phases within a cardiac cycle. Additional signal averaging of PC data might have offset any effects of cardiac pulsation on PC CBF. In PCASL, effects of cardiac noise are attenuated by repeated signal averaging for labeling durations that are greater than the R–R interval.[38] Future studies comparing these modalities with the availability of a "gold-standard" measure of CBF would be helpful. At the moment ^{15}O-PET is considered as a "gold-standard" and there are few small-scale studies that have shown good agreement between ASL and ^{15}O-PET CBF values,[39–41] but it would be desirable to have this comparison for a larger sample size with all three methods considered together.

CBF values obtained using PC were found to be significantly higher than those obtained using PCASL. This systematic difference could be due to either overestimation of CBF by PC due to partial volume effects, underestimation of CBF in PCASL MRI due to not achieving a labeling efficiency of 0.85, or some combination of these effects. It has been reported in prior literature[30,31] that partial volume effects can lead to significant overestimation of VFR in PC. On the other hand, use of $\alpha = 0.73$ rather than $\alpha = 0.85$ (as recommended in Alsop et al.[13]) would result in equal means of the distribution of the CBF values obtained using both the methods and would suggest that the PCASL labeling efficiency achieved in a large multisite study such as CARDIA may be somewhat lower than is typically assumed. The restriction of the segmented masks of the blood vessels to only those voxels in which the velocity values are positive also results in overestimation of blood flow, though this effect is expected to be small. PC MRI derives mean CBF by dividing total arterial flow by the brain volume measured using structural MRI, while in PCASL MRI, CBF is measured directly at the voxel level and then brain voxels are averaged to derive mean CBF. Differences in volume coverage of the brain could explain some of the variability between PC MRI and ASL MRI, but would not be expected to bias the difference in a systematic way. Incorrect assumptions for the values of other model parameters (e.g. average brain density, T1 of blood and blood:brain partition coefficient) can also contribute to a systematic difference. Because the labeling efficiency α enters the formula for CBF as a proportionality constant, correlations of other variables with CBF would be identical whether PCASL or PC is used, if α were the only factor that caused the two estimates to differ. However, correlations would differ between the two methods for categorical representations of CBF, such as the percentage with low CBF (which will be higher for CBF_{PCASL} than for CBF_{PC}).

CBF measured using PC was found to be higher and more variable in the Oakland site than in the Minneapolis site, though there were no significant site differences in any of the demographics or acquisition parameters. We currently do not have an explanation for the site effects seen in CBF_{PC}. On the other hand, no site differences were observed for CBF_{PCASL}. Because CBF_{PCASL} is derived from the difference between scans acquired with and without labeling, it is relatively resistant to biophysical effects that can affect quantification in other modalities. In addition, the PCASL labeling scheme was designed to be insensitive to the possible variability in velocity, B0 or B1 field. The observed site effects with PC also degraded the correlation between CBF_{PCASL} and CBF_{PC} in the Oakland site compared to the Minneapolis site.

We examined the ratio CBF_{PCASL}/CBF_{PC} as a function of the mean arterial flow velocity and did not find any evidence that the ratio decreases with increase in the flow velocity within this velocity range as has previously been reported.[15] Similar results were obtained when the mean velocity was replaced by the maximum arterial velocity. Indeed, we observed a subtle positive correlation indicating an increase in the labeling efficiency for increasing velocities, though this correlation was significant only for the mean velocity when the whole data set was considered. It should be noted that the maximum velocity is less sensitive to the errors in segmenting the arteries, as the voxel having the highest velocity is highly likely to fall within the segmented ROI for each artery. This trend of slight decrease in labeling efficiency for smaller velocities within this velocity range is consistent with the simulation results reported in Dai et al.[14] Discrepancies between our findings and the results reported in Aslan et al.[15] may be at least partly attributed to the fact that

Aslan et al.[15] examined data acquired under both normocarbia and hypercarbia, whereas the current study reflects only normocarbia, though the velocity ranges were comparable. Discrepancies between findings may also have resulted from slightly different locations for the labeling plane and the PC MRI plane in the two studies. Finally, the conclusions in Aslan et al.[15] were derived from a small sample (26 measurements), which can be biased by significant variability present in each modality as evidenced from our data. In summary, the data analyzed in the present study from a very large cohort do not support the conclusion that there is a significant velocity-dependent reduction in PCASL labeling efficiency, at least under normocapnia.

Although several studies, including our own,[19,22] have used CBF_{PC} as a means of calibrating PCASL labeling efficiency, the findings of the current study do not support this practice, at least for the specific PC methodology used. Most of the variability of the CBF_{PCASL} in the present study could not be explained by CBF_{PC}, and CBF_{PC} measurements were found to be more variable than CBF_{PCASL} measurements. While sex and age correlations in CBF consistent with prior reports[33,34] were observed in both PCASL and PC data, PCASL demonstrated similar but numerically higher correlations between CBF and sex or age than did PC, suggesting that PCASL measures might be more accurate. In addition, prior studies demonstrate that reproducibility in whole-brain CBF values using PC with repeated measurements[16] is a bit poorer than that reported for gray matter CBF using PCASL with repeated measurements.[42] PC also demonstrated significant site effects while PCASL did not. Finally, Figure 4(b) demonstrates that for a fixed value of CBF obtained using one modality, the other modality can demonstrate 2–3 fold differences in CBF values. Such differences are unlikely to reflect variations in PCASL labeling efficiency and are most likely attributed to simultaneous variability in both the methods.

This study was based on PCASL and PC data acquired as part of a multimodal neuroimaging protocol included in the CARDIA Year 25 dataset. Both PCASL and PC were successfully obtained in a large fraction of the subjects scanned. However, this scanning protocol also had technical limitations. Firstly, no time of flight angiogram was performed to visualize the ICAs and VAs for optimal placement of either the PCASL labeling plane or the PC imaging plane. Doing so might have reduced variability in PCASL labeling efficiency and increased the accuracy and yield of CBF_{PC} measurements. CBF_{PC} accuracy can further be improved by measuring flow in three directions since it is generally difficult to have all the arteries perpendicular to the imaging plane. Labeling efficiency in PCASL can also be further optimized by accounting for magnetic field shifts at the labeling plane,[43] though this procedure is time consuming. Secondly, while PCASL data were signal averaged over several minutes, PC data were acquired over approximately one minute. Additional signal acquisition and averaging might improve the reliability of the CBF_{PC} measurements. Thirdly, CBF_{PCASL} modeling utilized a modified single compartment model with a single post-labeling delay and an assumed value for blood T1 as was recently recommended for clinical applications.[13] More complex modeling incorporating arterial transit time, blood and brain compartments, brain T1 mapping, and blood sampling for hematocrit might have further increased the accuracy of CBF_{PCASL}. No large multisite study to date has achieved this level of complexity in MRI CBF measurement, but a precedent for achieving both high throughput and high-complexity scanning is now being set by the Human Connectome Project.

In conclusion, CBF is found to have high inter-subject variation across a large cohort of middle-aged subjects representative of the general population, and this variability was confirmed by both modalities. Although CBF values were highly significantly correlated between modalities, over half of the observed method variance was not explained, illustrating that both methods are noisy at the level of individual subject measurements. Although the notion of using PC to calibrate PCASL MRI is appealing, the present data do not support this practice as a means of increasing the accuracy of CBF_{PCASL} estimation.

Funding

The Coronary Artery Risk Development in Young Adults Study (CARDIA) is supported by contracts HHSN268201300025C, HHSN268201300026C, HHSN268201300027C, HHSN268201300028C, HHSN268201300029C, and HHSN268200900041C from the National Heart, Lung, and Blood Institute and the Intramural Research Program of the National Institute on Aging. This study was further supported by grants from the National Institutes of Health, namely EB015893, MH080729. .

Acknowledgements

The authors would like to acknowledge Alex Smith for her help in data processing and Dr. Kiang Liu for his valuable comments.

Declaration of conflicting interests

The author(s) declared no potential conflicts of interest with respect to the research, authorship, and/or publication of this article.

Authors' contributions

Sudipto Dolui: Processed ASL data, developed PC-MRI analysis utility, compiled the results and prepared the manuscript.

Ze Wang: Processed ASL data, provided support for ASLtoolbox, critical review of manuscript.
Danny JJ Wang: Developed ASL sequence and the design for comparison with PC MRI, critical review of manuscript.
Raghav Mattay: Segmented the arteries in PC-MRI scans.
Mack Finkel: Did preliminary analysis of PC-MRI scans.
Mark Elliott: Implemented scanning protocols.
Lisa Desiderio: Data coordination.
Ben Inglis: MRI field site coordinator.
Bryon Mueller: MRI field site coordinator.
Randall B Stafford: Did preliminary analysis of PC-MRI scans, created PC-MRI analysis GUI prototype.
Lenore J Launer: Designed and obtained funding for the CARDIA Brain MRI Sub-study, critical review of manuscript.
David R Jacobs Jr: Participated in data analysis, critical review of manuscript.
R Nick Bryan: Supervised data acquisition, participated in data analysis, critical review of manuscript.
John A. Detre: Supervised methods, analysis, and manuscript preparation.

References

1. Jain V, Langham MC and Wehrli FW. MRI estimation of global brain oxygen consumption rate. *J Cereb Blood Flow Metab* 2010; 30: 1598–1607.
2. Kety SS and Schmidt CF. The determination of cerebral blood flow in man by the use of nitrous oxide in low concentrations. *Am J Physiol* 1945; 143: 53–66.
3. Herscovitch P, Markham J and Raichle ME. Brain blood flow measured with intravenous H2(15)O. I. Theory and error analysis. *J Nucl Med* 1983; 24: 782–789.
4. Dagal A and Lam AM. Cerebral blood flow and the injured brain: how should we monitor and manipulate it? *Curr Opin Anaesthesiol* 2011; 24: 131–137.
5. Detre JA, Wang J, Wang Z, et al. Arterial spin-labeled perfusion MRI in basic and clinical neuroscience. *Curr Opin Neurol* 2009; 22: 348–355.
6. Williams DS, Detre JA, Leigh JS, et al. Magnetic resonance imaging of perfusion using spin inversion of arterial water. *Proc Natl Acad Sci U S A* 1992; 89: 212–216.
7. Detre JA, Leigh JS, Williams DS, et al. Perfusion imaging. *Magn Reson Med* 1992; 23: 37–45.
8. Zhang W, Williams DS, Detre JA, et al. Measurement of brain perfusion by volume-localized NMR spectroscopy using inversion of arterial water spins: accounting for transit time and cross-relaxation. *Magn Reson Med* 1992; 25: 362–371.
9. Detre JA, Zhang W, Roberts DA, et al. Tissue specific perfusion imaging using arterial spin labeling. *NMR Biomed* 1994; 7: 75–82.
10. Alsop DC and Detre JA. Reduced transit-time sensitivity in noninvasive magnetic resonance imaging of human cerebral blood flow. *J Cereb Blood Flow Metab* 1996; 16: 1236–1249.
11. Buxton RB, Frank LR, Wong EC, et al. A general kinetic model for quantitative perfusion imaging with arterial spin labeling. *Magn Reson Med* 1998; 40: 383–396.
12. Wong EC, Buxton RB and Frank LR. A theoretical and experimental comparison of continuous and pulsed arterial spin labeling techniques for quantitative perfusion imaging. *Magn Reson Med* 1998; 40: 348–355.
13. Alsop DC, Detre JA, Golay X, et al. Recommended implementation of arterial spin-labeled perfusion MRI for clinical applications: a consensus of the ISMRM perfusion study group and the European consortium for ASL in dementia. *Magn Reson Med* 2015; 73: 102–116.
14. Dai W, Garcia D, de Bazelaire C, et al. Continuous flow-driven inversion for arterial spin labeling using pulsed radio frequency and gradient fields. *Magn Reson Med* 2008; 60: 1488–1497.
15. Aslan S, Xu F, Wang PL, et al. Estimation of labeling efficiency in pseudocontinuous arterial spin labeling. *Magn Reson Med* 2010; 63: 765–771.
16. Spilt A, Box FM, van der Geest RJ, et al. Reproducibility of total cerebral blood flow measurements using phase contrast magnetic resonance imaging. *J Magn Reson Imaging* 2002; 16: 1–5.
17. Bakker CJ, Hartkamp MJ and Mali WP. Measuring blood flow by nontriggered 2D phase-contrast MR angiography. *Magn Reson Imaging* 1996; 14: 609–614.
18. Jung Y, Wong EC and Liu TT. Multiphase pseudocontinuous arterial spin labeling (MP-PCASL) for robust quantification of cerebral blood flow. *Magn Reson Med* 2010; 64: 799–810.
19. Vidorreta M, Wang Z, Rodriguez I, et al. Comparison of 2D and 3D single-shot ASL perfusion fMRI sequences. *Neuroimage* 2013; 66: 662–671.
20. Leenders KL, Perani D, Lammertsma AA, et al. Cerebral blood flow, blood volume and oxygen utilization. Normal values and effect of age. *Brain* 1990; 113(Pt 1): 27–47.
21. Rodriguez G, Warkentin S, Risberg J, et al. Sex differences in regional cerebral blood flow. *J Cereb Blood Flow Metab* 1988; 8: 783–789.
22. Jain V, Duda J, Avants B, et al. Longitudinal reproducibility and accuracy of pseudo-continuous arterial spin labeled perfusion MR imaging in typically developing children. *Radiology* 2012; 263: 527–536.
23. Wang Z, Aguirre GK, Rao H, et al. Empirical optimization of ASL data analysis using an ASL data processing toolbox: ASLtbx. *Magn Reson Imaging* 2008; 26: 261–269.
24. Wang Z. Improving cerebral blood flow quantification for arterial spin labeled perfusion MRI by removing residual motion artifacts and global signal fluctuations. *Magn Reson Imaging* 2012; 30: 1409–1415.
25. Wang J, Zhang Y, Wolf RL, et al. Amplitude-modulated continuous arterial spin-labeling 3.0-T perfusion MR imaging with a single coil: Feasibility study. *Radiology* 2005; 235: 218–228.
26. Lu H, Clingman C, Golay X, et al. Determining the longitudinal relaxation time (T1) of blood at 3.0 Tesla. *Magn Reson Med* 2004; 52: 679–682.
27. Silvennoinen MJ, Kettunen MI and Kauppinen RA. Effects of hematocrit and oxygen saturation level on blood spin-lattice relaxation. *Magn Reson Med* 2003; 49: 568–571.

28. Eggert LD, Sommer J, Jansen A, et al. Accuracy and reliability of automated gray matter segmentation pathways on real and simulated structural magnetic resonance images of the human brain. *PloS One* 2012; 7: e45081.
29. Brett M, Johnsrude IS and Owen AM. The problem of functional localization in the human brain. *Nat Rev Neurosci* 2002; 3: 243–249.
30. Lagerstrand KM, Lehmann H, Starck G, et al. Method to correct for the effects of limited spatial resolution in phase-contrast flow MRI measurements. *Magn Reson Med* 2002; 48: 883–889.
31. Tang C, Blatter DD and Parker DL. Correction of partial-volume effects in phase-contrast flow measurements. *J Magn Reson Imaging* 1995; 5: 175–180.
32. Hamilton CA. Correction of partial volume inaccuracies in quantitative phase contrast MR angiography. *Magn Reson Imaging* 1994; 12: 1127–1130.
33. Lotz J, Meier C, Leppert A, et al. Cardiovascular flow measurement with phase-contrast MR imaging: basic facts and implementation. *Radiographics* 2002; 22: 651–671.
34. Paulson OB, Strandgaard S and Edvinsson L. Cerebral autoregulation. *Cerebrovasc Brain Metabol Rev* 1990; 2: 161–192.
35. Giller CA. A bedside test for cerebral autoregulation using transcranial Doppler ultrasound. *Acta Neurochir (Wien)* 1991; 108: 7–14.
36. Florence G and Seylaz J. Rapid autoregulation of cerebral blood flow: a laser-Doppler flowmetry study. *J Cereb Blood Flow Metab* 1992; 12: 674–680.
37. Zhang R, Zuckerman JH, Giller CA, et al. Transfer function analysis of dynamic cerebral autoregulation in humans. *Am J Physiol* 1998; 274(1 Pt 2): H233–H241.
38. Wu WC, Edlow BL, Elliot MA, et al. Physiological modulations in arterial spin labeling perfusion magnetic resonance imaging. *IEEE Transac Med imaging* 2009; 28: 703–709.
39. Ye FQ, Berman KF, Ellmore T, et al. H(2)(15)O PET validation of steady-state arterial spin tagging cerebral blood flow measurements in humans. *Magn Reson Med* 2000; 44: 450–456.
40. Xu G, Rowley HA, Wu GM, et al. Reliability and precision of pseudo-continuous arterial spin labeling perfusion MRI on 3.0 T and comparison with 15O-water PET in elderly subjects at risk for Alzheimer's disease. *NMR Biomed* 2010; 23: 286–293.
41. Zhang K, Herzog H, Mauler J, et al. Comparison of cerebral blood flow acquired by simultaneous [15O]water positron emission tomography and arterial spin labeling magnetic resonance imaging. *J Cereb Blood Flow Metab* 2014; 34: 1373–1380.
42. Chen Y, Wang DJ and Detre JA. Test-retest reliability of arterial spin labeling with common labeling strategies. *J Magn Reson Imaging* 2011; 33: 940–949.
43. Shin DD, Liu TT, Wong EC, et al. Pseudocontinuous arterial spin labeling with optimized tagging efficiency. *Magn Resona Med* 2012; 68: 1135–1144.